III - 399

ELASTO-PLASTIC ANALYSIS OF STATIC AND DYNAMIC ACTIVE EARTH PRESSURE AGAINST RIGID RETAINING WALL

Hemanta Hazarika, Nagoya University
Hiroshi Matsuzawa, Nagoya University
Masahiro Sugimura, Nagoya University

INTRODUCTION: Recent experimental studies by various researchers in the field of earth pressure have demonstrated that the nature and the magnitude of the static and the dynamic earth pressure and the point of application of the resultant depends to a great extent on the kinds of movement the retaining wall experiences as well as the acceleration level of the ground motion. However, the numerical treatment to examine this dependancy is lagging behind. Hence an elasto-plastic numerical analysis has been performed to add momentum in this direction.

INTERFACE MODELLING: The analytical model shown in the Fig. 1 is the simulation of the experimental model developed by Ichihara and Matsuzawa(1973). Idealised interface elements having bilinear stress-displacement relationship with only a shear spring shown in the Fig. 2 were introduced between the wall and the soil interface. The relative displacement between the wall and the soil is kept zero during the analysis by providing equal forced displacement to both the wall nodes as well as the soil element nodes, thus avoiding the separation of the wall and soil.

CONSTITUTIVE RELATION: Using the Drucker-Prager type of yield function, along with the assumption of associated flow rule, the following constitutive equation can be derived,

$$d\sigma_{ij} = [D^e_{ijkl} - \frac{D^e_{ijmn}(\mathbf{m}+\beta\mathbf{n})(\mathbf{m}+\alpha\mathbf{n})D^e_{vwkl}}{h+(\mathbf{m}+\alpha\mathbf{n})D^e_{pqrs}(\mathbf{m}+\beta\mathbf{n})}]d\epsilon_{ij} \quad (1)$$

Here $\mathbf{m} = s_{ij}/s$,where $s = \sqrt{s_{ij}s_{ij}}$ and $\mathbf{n} = \frac{\mathbf{I}}{\sqrt{3}}$.

s_{ij} is the deviatoric part of the stress tensor σ_{ij} , I is the unit tensor. β is the dilatancy factor and α is the material constant . D^e_{ijkl} is the elastic stress-strain matrix, h is the hardening parameter.

RESULTS AND DISCUSSION: Four kinds of movement of the wall is considered: namely translation(T), roatation about the base(RB), rotation about the top(RT) and rotation about the base as well as translation(RB-T) in which case the center of rotation is 20 cm below the base of the wall. The computed distribution of the earth pressure in Fig. 3(a)-3(d) show that the distribution pattern differs depending on the wall movement modes. Fig 4 shows the variations of the coefficient of earth pressure K, friction angle coefficient $\tan\delta$ and the relative height of point of application h/H with wall displacement for the RT mode.

Active state is defined at that point when the soil elements in the backfill reach the critical state forming either a clear failure wedge or a slip surface. The displacement required to reach this point is found to be larger than at the point of maximum value of $\tan\delta$, experimentally defined to be the active state. The corresponding $(h/H)_A$ is found to vary with the angle of internal friction ϕ of the backfill as shown in the Fig. 5. It can also be observed that the trend of the variation is different for each case of the wall movement mode.

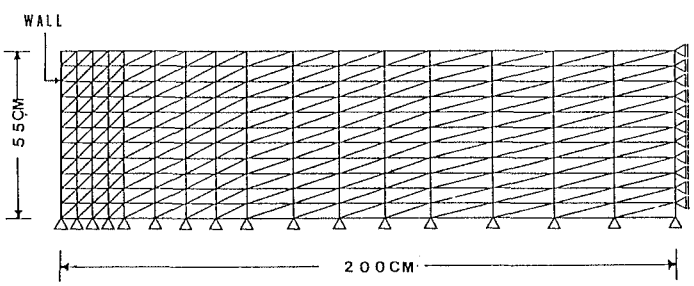

Fig. 1: Analytical Model

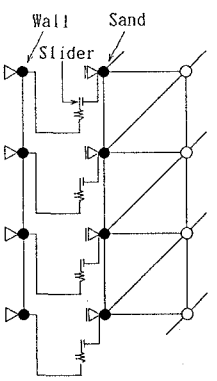

Fig. 2: Idealised Interface Model

Dynamic analysis also has been performed for the same model for the RB-T mode by time domain analysis. Fig. 6 shows the variation of the earth pressure with mean wall displacement. The effect of inertia in this case results in a distribution pattern different from that of the static case at the upper part of the backfill. The variations of K, $\tan\delta$ and h/H in the Fig. 7 for both the experimental and the analytical results show that though at the initial stage both the results agree resonably, with increase of displacement they deviate, may be due to discontinuity of the stress at the critical state. The Fig. 8 shows the variations of K, $\tan\delta$ and h/H at the active state with different values of the acceleration. It can be observed that the analytical results agree well with the experimental results except for the case of $\tan\delta$, which may be due to our assumption of bilinear behavior of interface elements.

CONCLUSION: Unlike Coulomb's pressure as well as Mononobe-Okabe's pressure, the distribution of earth pressure is *nonlinear* and hence the relative height h/H is not unique value. It depends on mode of movement of wall, material parameters like the angle of internal friction ϕ and the acceleration of the ground. It is not necessary to reduce the value of ϕ for the calculation of the Mononobe-Okabe's pressure under the maximum inertia force as suggested by some researchers. The unexpected drop of $\tan\delta$ value after the maximum point may be due to the absence of interface elements at the bottom as well as right side of the analytical model.

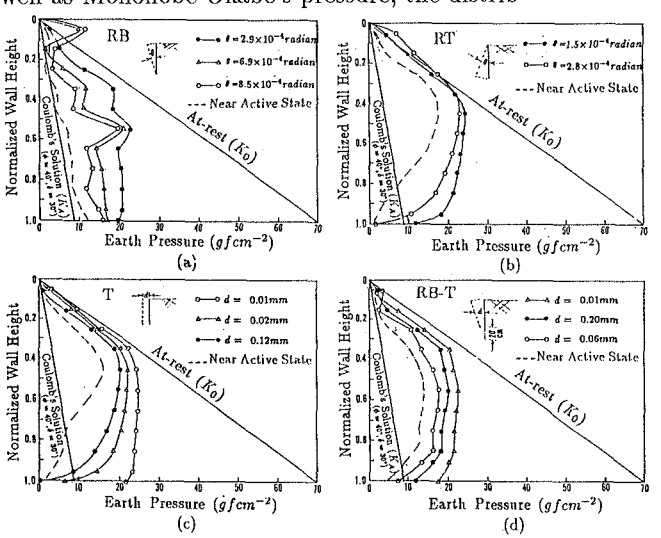

Fig. 3: Distribution of Earth Pressure behind the Wall.

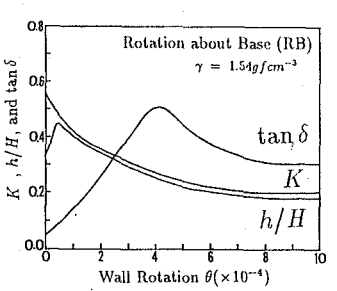

Fig. 4: Variations of K, h/H, and $\tan\delta$

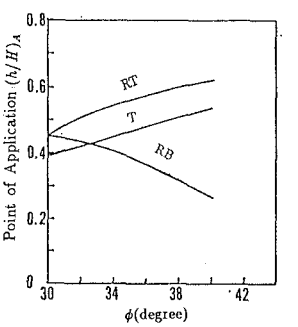

Fig. 5: Variations of $(h/H)_A$ with ϕ

References

[1] Ichihara, M., and Matsuzawa, H., "Earth Pressure During Earthquake", *Soils and Foundations*, JSSMFE, Vol. 13, No. 4, 1973, pp. 75-86.

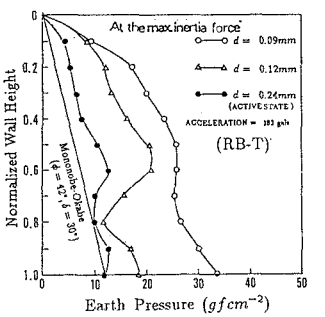

Fig. 6: Distribution of Earth Pressure

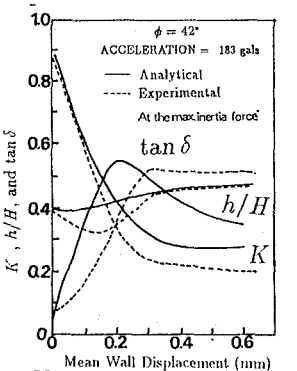

Fig. 7: Variations of K, h/H, and $\tan\delta$

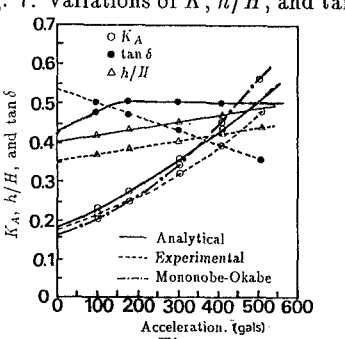

Fig. 8